NEW ADVANCES IN BORON SOIL CHEMISTRY

Sabine Goldberg[1] and Chunming Su[2]

[1] Corresponding Author
USDA-ARS
George E. Brown, Jr., Salinity Laboratory
450 W, Big Springs Road
Riverside, California 92507
USA
Phone: 951-369-4820
Fax: 951-342-4962
Email: sgoldberg@ussl.ars.usda.gov

[2] USEPA
National Risk Management Research Laboratory
919 Kerr Research Drive
Ada, Oklahoma 74820
USA

20 Pages
0 Tables
17 Figures

ABSTRACT

Boron is an essential plant micronutrient for which the range between deficiency and toxicity is narrower than for any other nutrient element. Plants respond directly to the amount of B in soil solution and only indirectly to the amount of B adsorbed on soil particle surfaces. Therefore the adsorption complex acts as both a source and a sink for B and can attenuate phytotoxic soil solution B concentrations. Many aspects of B soil chemistry play an important role in governing plant B response. These include: methodologies for determining the mechanisms of B attachment to soil particle surfaces, kinetics of B desorption reactions, description and prediction of B adsorption reactions using chemical models, use of B soil tests to predict plant response in field situations. A detailed understanding of B adsorption behavior is necessary to gain an accurate assessment of soil solution B concentrations that is essential for predicting plant response. Indirect and direct experimental procedures have been used to determine the mode of B attachment to soil particle surfaces. Accurate characterization of the desorption reactions that release B into soil solution is also important. Many modeling approaches exist for describing B adsorption reactions on soils and soil minerals. To evaluate management options for high B soils and waters, a model that can predict solution B concentrations is needed. Boron soil tests need to be tested for their ability to predict soil solution B concentrations under conditions of potential B toxicity, especially in field situations.

INTRODUCTION

Boron is an essential micronutrient element required for plant growth. Boron deficiency is wide-spread in crop plants throughout the world especially in coarse-

textured soils in humid areas. Boron toxicity can also occur, especially in arid regions under irrigation. Plants respond directly to the B concentration in soil solution and only indirectly to the amount of B attached to soil surfaces (Keren et al., 1985). Therefore, the soil adsorption complex acts as both a source and a sink for dissolved B and can mitigate phytotoxic soil solution B concentrations.

The primary B adsorbing surfaces in soils are: aluminum and iron oxides, clay minerals, calcium carbonate, and organic matter (Goldberg, 1997). Boron adsorption on all of these surfaces increases with increasing solution pH, reaches an adsorption maximum near pH 8 to 9, and decreases with further increases in solution pH. The mechanism of B adsorption on these surfaces is considered to be ligand exchange with reactive surface hydroxyl groups leading to strong specific adsorption.

In addition to solution pH, other factors affecting the availability of B in soils are: soil texture, soil moisture, and soil temperature (Goldberg, 1997). Fine-textured soils usually contain more available B than coarse-textured soils because of their greater content of clay minerals (Gupta, 1968). Boron is generally less available in dry soil and increases with increasing temperature (Fleming, 1980).

Plant B response is affected by many aspects of B soil chemistry. In this review we will treat several of these topics: i) methodologies for determining the mechanisms of B attachment to soil particle surfaces; ii) kinetics of B desorption reactions; iii) description and prediction of B adsorption reactions using chemical models; iv) use of B soil tests to predict plant response in field situations.

DETERMINING BORON ATTACHMENT TO SOIL SURFACES

To accurately describe the adsorption behavior of B in soils, the mode of

attachment of B to soil particles must be known. Indirect and direct experimental procedures have been used to establish B adsorption mechanisms on oxide minerals. Indirect methods include point of zero charge (PZC) shifts and ionic strength dependence. Direct observation of ion adsorption mechanisms is provided by a variety of spectroscopic techniques.

Electrophoretic mobility measures that movement of charged particles in an applied electric field. Lack of mobility indicates the PZC of the particles. Inner-sphere surface complexes are strong, specific, and contain no water between the adsorbing ion and the point of surface attachment. Inner-sphere anion adsorption shifts the PZC to lower values and causes reversals of electrophoretic mobility with increasing anion concentration (Hunter, 1981). Adsorption of B lowered the PZC of an aluminum oxide mineral, gibbsite (see Figure 1) providing indirect evidence of strong, specific, inner-sphere adsorption.

Ionic strength dependence of adsorption can be used to distinguish inner- and outer-sphere surface complexes. Outer-sphere surface complexes are weaker, nonspecific, and contain at least one water molecule between the adsorbing ion and the point of surface attachment. Decreasing adsorption with increasing solution ionic strength is considered evidence for outer-sphere surface complexation; while ions showing little ionic strength dependence or increasing adsorption with increasing ionic strength are considered to form inner-sphere surface complexes (McBride, 1997). Boron adsorption on an iron oxide mineral, goethite (see Figure 2) showed little ionic strength dependence, suggesting inner-sphere surface complex formation.

Infrared spectroscopy is a technique that can provide insight into the type and number of bonds that an adsorbed ion forms with the solid surface. Attenuated total

reflectance Fourier transform infrared (ATR-FTIR) spectroscopy can be used to observe the attachment of surface adsorbed ions in the presence of water. This is critical for applicability to natural systems such as soils.

Su and Suarez (1995) studied mechanisms of boron adsorption on amorphous aluminum and iron hydroxides using ATR-FTIR. Samples for ATR-FTIR spectroscopy consisted of either pure boric acid in 0.1 M NaCl or mineral pastes obtained from centrifugation of equilibrated suspensions. Four boric acid solutions (4.62, 9.25, 23.1, and 92.5 mmol L^{-1} in 0.1 M NaCl) were prepared from CO_2-free water and were adjusted to pH 7, 9, 10 and 11 with 1.0 M NaOH (CO_2-free). Mineral suspensions consisted of 0.25 g of either am-$Al(OH)_3$ or am-$Fe(OH)_3$ in 12.5 mL of 0.1 M NaCl adjusted to desired pH values near 7 and 10 and initial B concentrations (4.62, 9.25 and 23.1 mmol L^{-1}). Suspensions of am-$Fe(OH)_3$ were equilibrated for 20 h at 25^{o}C and suspensions of am-$Al(OH)_3$ were equilibrated at pH 10.2 ± 0.1 and 5^{o}C. It was found in a preliminary experiment that at a pH value greater than 8.6 at 25^{o}C, am-$Al(OH)_3$ had been largely transformed to pseudoboehmite and bayerite via X-ray diffraction examination, but remained amorphous at 5^{o}C for pH 3 to 11 after 20 h equilibration. Suspensions were centrifuged for 30 min at the corresponding temperature. The B concentration in the supernatant was determined using a Technicon Autoanalyzer II and the azomethine-H method described by Bingham (1982).

Infrared spectroscopic analysis of boric acid solutions was performed with the reservoir module and analysis of mineral pastes with the pressure plate module of the horizontal ATR accessory using horizontal ATR and an internal reflectance element (IRE) of ZnSe crystal. Detailed experimental procedures can be found in Su and Suarez (1995). All ATR-FTIR spectra were recorded from 4000 to 700 cm^{-1} at 4 cm^{-1} over

1000 scans.

To obtain signals of B, the spectra of the pH-adjusted 0.1 M NaCl solution or mineral paste without B (reference) were subtracted from the spectra of the 0.1 M NaCl solution or paste with added B at the same pH (sample), both previously ratioed against the spectrum of the empty cell (background), respectively. A subtraction factor of 1.000 was used.

Boric acid is a neutral trigonal molecule. It is a very weak monobasic Lewis acid that accepts a hydroxyl ion to form the tetrahedral borate anion as indicated in Figure 3. The pK_a of boric acid is 9.24 (Bassett, 1980). Figure 4 shows the ATR-FTIR spectra of an aqueous B solution as a function of solution pH. The peak assignments are as follows: 1410 cm^{-1}, B-O asymmetric stretching of trigonal B, 955 cm^{-1}, asymmetric stretching of tetrahedral B, 1148-1170 cm^{-1}, mixture of B-OH bending of trigonal and tetrahedral B (Su and Suarez, 1995).

ATR-FTIR difference spectra of am-$Al(OH)_3$ paste at pH 6.8 ± 0.2 with adsorbed B are shown in Figure 5a for three initial B concentrations of 4.62, 9.25 and 23.1 mmol L^{-1}. The equilibrium B concentrations are far lower than the initial concentrations and are plotted next to the spectra in Figure 5a. A broad band centered at 1420 cm^{-1} is assigned to trigonal boron asymmetric stretching mode and a band at 1280 cm^{-1} is assigned to trigonal boron B-OH bending mode. Up shift of both bands to higher frequencies in the mineral paste was evident compared to the pure boric acid solution (1410 and 1148 cm^{-1}) at pH 7. This is attributed to the strengthening of O-B and B-OH bonds in the surface complex -Al-O-$B(OH)_2$ when the boric acid molecule is complexed with surface functional groups such as -Al-OH. The intensity of these bands increased with increasing boron adsorption. Figure 5b shows the ATR-FTIR difference spectra of

an am-$Al(OH)_3$ paste with and without added B at pH 10.2 ± 0.1 and 5^oC. A band at 1412 cm^{-1} (B-O asymmetric stretching of trigonal B) was not significantly shifted compared to the 1410 cm^{-1} band for boric acid solution at pH 7; however, the B-OH bending of trigonal B band had a narrower width and was shifted to a higher frequency of 1266 cm^{-1} from 1148 cm^{-1} due to the formation of surface B complexes. Surface complexation is likely to make the B-OH bond stronger so as to increase the B-OH bending frequency. Characterization of tetrahedral B at the mineral surface was not successful because of severe band interference in the range of 1000-900 cm^{-1} from the Al-O bond that shows strong absorbance centered at 969 cm^{-1}. Boric acid solution spectra show tetrahedral boron as the dominant species at pH 10.2 ± 0.1 (Figure 4c); however, tetrahedral boron may not necessarily be the dominant adsorbed species on am-$Al(OH)_3$ surfaces at pH 10.2. This may be explained by the change of surface charge of minerals as a function of pH. Am-$Al(OH)_3$ is expected to be negatively charged at pH 10.2 and the neutral $B(OH)_3$ species could be preferred due to its higher affinity for the negatively charged surface of am-$Al(OH)_3$ at high pH; whereas, the $B(OH)_4^-$ ion would encounter charge repulsion. Another possibility is that polymerization of adsorbed B species occurred, resulting in both trigonally and tetrahedrally coordinated B.

Figure 6 shows the ATR-FTIR difference spectra of amorphous iron oxide with and without B (Su and Suarez, 1995). The asymmetric stretching of trigonal B was shifted downward while the B-OH binding was shifted upward. A weak tetrahedral B asymmetric stretching band was shifted upward and evident at 962 and 985 cm^{-1}. Shifts in frequency are indicative of surface complexation of B. A similar study of B adsorption onto amorphous iron oxide (Peak et al., 2003) assigned the 1395 cm^{-1} band

to outer-sphere surface complexation and the 990, 1250, and 1330 cm^{-1} bands to inner-sphere surface complexation of trigonal B (Figure 7).

Based on both macroscopic and microscopic results, B forms strong inner-sphere complexes on the soil minerals: amorphous iron oxide, amorphous aluminum oxide, and allophane (Su and Suarez, 1997). Boron also forms weak outer-sphere complexes on amorphous iron oxide. This physically bound B could be readily leached and would be available for plant uptake.

KINETICS OF BORON DESORPTION REACTIONS

Boron containing minerals generally do not control B solubility in soil solution because they are either too insoluble (tourmaline) or too soluble (hydrated B minerals). The amount of B in soil solution is usually controlled by B adsorption-desorption reactions (Goldberg, 1997). In many soils, B adsorption is readily reversible and the B desorption isotherm corresponds closely to the B adsorption isotherm. Other soils exhibit hysteresis, the lack of correspondance of the B desorption isotherm with the B adsorption isotherm. The apparent irreversibility of B sorption has been attributed to conversion of readily desorbable monodentate B surface complexes into less readily desorbable bidentate complexes, incorporation of B into tetrahedral sites of clay minerals, and B diffusion into particle interiors.

Excess soluble B in arid land soils has often been attributed to the weathering of B containing minerals. Su and Suarez (2004) studied the release of boron from representative minerals and soils. They included two specimen illites (Morris and Fithian), two shales (Salt Creek and Moreno Gulch), a fresh and a weathered serpentine (antigorite) from the Coastal Range of California, a Traver silt loam and a Twisselman

clay loam both containing illite, chlorite, and palygorskite. The soils were collected from the San Joaquin Valley of California, USA. All samples were subjected to successive extraction (7 to 26 times) following each 12-h equilibration in 0.1 M (first three extraction) and 0.01 M $CaCl_2$ solution (subsequent extractions) until the supernatant B solutions were below the detection limit of 0.001 mmol B L^{-1}. Boron release from various minerals is depicted in Figure 8. After the successive washing to remove surface-adsorbed boron, the < 2 μm and 2-20 μm size fractions were separated and reacted in deionized water at pH 5, 7, and 9 adjusted with HCl and NaOH for up to 180 days. Effect of particle size, solution pH, and time on B concentration and B release for the two San Joaquin Valley soils is shown in Figure 9. Boron release rates decreased with equilibration time and increasing pH. Reclamation of high B soils may be followed by continued release of sparingly soluble sources of B. Knowledge of long-term B leaching from high B irrigated soils is essential for prediction of future B contamination of drainage waters in such places as the San Joaquin Valley of California, USA. The presence of illite, chlorite, and palygorskite minerals was found to be responsible for the long-term release of B in these soils (Su and Suarez, 2004). Boron release rates were highest for the smallest particles and the lowest solution pH (Su and Suarez, 2004). The long-term release rates can be used to predict B concentration in the field. Weathering of such soils may produce toxic levels of B within a few years following reclamation unless continued leaching is maintained.

PREDICTION OF BORON ADSORPTION USING CHEMICAL MODELS

Various modeling approaches have been used to describe B adsorption on soil minerals and soils. Empirical models such as the Freundlich and Langmuir adsorption

isotherms produce parameters that are only valid for the conditions under which the experiment was conducted. The Keren model (Keren and Mezuman, 1981) is a phenomenological equation that can describe B adsorption on soil minerals and soils as a function of solution pH. Yet it is empirical in that no physical significance can be attributed to the parameter values.

Chemical surface complexation models such as the constant capacitance model and the triple layer model define surface species, chemical reactions, mass balances, and charge balance and contain molecular features that can be given thermodynamic significance. The triple layer model has been used to describe B adsorption by soils in only one study (Goldberg, 2005) because of the difficulty in determining meaningful values for its large set of adjustable parameters. The constant capacitance model contains a much smaller number of adjustable parameters than the triple layer model and is therefore more suitable for describing adsorption on complex natural materials such as soils.

The constant capacitance model assumes that B adsorption occurs via a ligand exchange mechanism with reactive surface hydroxyls forming inner-sphere surface complexes. The placement of ions in the constant capacitance model is depicted in Figure 10. A detailed discussion of the theory, assumptions, and equations of the constant capacitance model is provided in Goldberg (1992). In the application of the constant capacitance model to B adsorption the following surface complexation reactions for the surface functional group, SOH, are defined:

$$SOH + H^+ \leftrightarrow SOH_2^+ \quad (1)$$

$$SOH \leftrightarrow SO^- + H^+ \quad (2)$$

$$SOH + H_3BO_3 \leftrightarrow SH_3BO_4^- + H^+ \quad (3)$$

SOH represents a reactive surface hydroxyl group on an oxide mineral or an aluminol or silanol group on the edge of a clay mineral. The equilibrium constant expressions for the above reactions are:

$$K_{+}(\text{int}) = \frac{[SOH_2^+]}{[SOH][H^+]}\exp(F\psi / RT) \quad (4)$$

$$K_{-}(\text{int}) = \frac{[SO^-][H^+]}{[SOH]}\exp(-F\psi / RT) \quad (5)$$

$$K_{B-}(\text{int}) = \frac{[SH_3BO_4^-][H^+]}{[SOH][H_3BO_3]}\exp(-F\psi / RT) \quad (6)$$

where F is the Faraday constant (C mol_c^{-1}), ψ is the surface potential (V), *R* is the molar gas constant (J mol^{-1} K^{-1}), *T* is the absolute temperature (K) and square brackets indicate concentrations (mol L^{-1}). The electrostatic potential term, exp(Fψ/RT), can be considered as a solid phase activity coefficient that corrects for surface charge.

Boron adsorption experiments on soils were carried out in batch systems to determine adsorption isotherms (amount of B adsorbed as a function of equilibrium solution B concentration) and adsorption envelopes (amount of B adsorbed as a function of solution pH at a fixed total B concentration). The soils were chosen to provide a wide range of soil chemical characteristics. Additional experimental details are provided in Goldberg et al. (2000). The constant capacitance model was able to describe B adsorption both as a function of solution B concentration and solution pH. The constant capacitance model was well able to fit B adsorption on 17 soils from the southwestern USA. Examples of model fit are shown in Figure 11 for two soils from California, USA.

A general regression model was developed to obtain soil surface complexation constants to allow prediction of B adsorption on additional soils using the constant

capacitance model. The model surface complexation constants were obtained from easily measured soil chemical properties: surface area (SA), organic carbon content (OC), inorganic carbon content (IOC), and free aluminum oxide content (Al). These parameters are also soil properties that correlate with soil B adsorption capacity. Experimental details for these chemical measurements are provided in Goldberg et al. (2000). The prediction equations for obtaining the surface complexation constants are:

$$LogK_{B-} = -9.14 - 0.375\ln(SA) + 0.167\ln(OC) + 0.111\ln(IOC) + 0.466\ln(Al) \quad (7)$$

$$LogK_{+} = 7.85 - 0.102\ln(OC) - 0.198\ln(IOC) - 0.622\ln(Al) \quad (8)$$

$$LogK_{-} = -11.97 + 0.302\ln(OC) + 0.0584\ln(IOC) + 0.302\ln(Al) \quad (9)$$

Additional details on the statistical analysis are provided in Goldberg et al. (2000).

The prediction equations were used to predict surface complexation constants for other soils that had not been used to obtain the regression model. Using these predicted constants, the constant capacitance model was well able to predict B adsorption behavior by 37 diverse soils from both the Southwestern (Goldberg et al., 2000, see Figure 12) and Midwestern (Goldberg et al., 2004, see Figure 13) parts of the USA. This approach represents a completely independent evaluation of the ability of the model to predict B adsorption using zero adjustable parameters. These results suggest widespread applicability of the prediction approach for describing B adsorption behavior in soils both as a function of solution B concentration and solution pH. The prediction equations have been incorporated into the UNSATCHEM speciation-transport computer program (Suarez and Simunek, 1997) to allow prediction of soil solution B concentrations for different soils and chemical conditions without the need for detailed characterization of B adsorption.

USE OF BORON SOIL TESTS TO PREDICT PLANT RESPONSE

A wide variety of soil tests has been developed to predict plant B content. The most common soil test for estimating plant available B is hot-water-soluble (Berger and Truog, 1940). Calcium chloride-mannitol (Cartwright et al., 1983) and ammonium acetate (Gupta and Stewart, 1975) extracts have also been used extensively. A DTPA-sorbitol extractant has been recommended by the North American Proficiency Testing Program to estimate the potential soil bioavailability of Zn, Cu, Mn, Fe, and B (Miller et al., 2000). All of these soil tests have been found to be highly correlated (Goldberg et al., 2002).

Historically, B soil tests have been developed to predict B deficient soils and have not generally been evaluated for their ability to predict soil conditions that produce B toxicity effects in plants. Shallow groundwater usage by crops improves irrigation efficiency and is being tested in the San Joaquin Valley of California, USA. Such management systems have the potential to adversely affect crop yields due to build-up of soil solution salinity and B concentration. Several soil B extractants were used to determine B uptake by field and container grown plants. The extractants were evaluated for their ability to predict B content of both field-grown and container-grown plants under conditions of potential B toxicity (Goldberg et al., 2002, 2003).

For the container study, a heavy clay soil was collected from the Broadview Water District in the San Joaquin Valley of California, USA. Subsamples of soil were treated to attain seven different B levels replicated four times. Muskmelon (*Cucumis melo* L.) variety *Top Mark* was planted in outdoor containers in a randomized block design and fertilized and irrigated as needed. Plant leaves were sampled prior to fruit set and at harvest; stems and fruits were sampled at harvest only. Soils were sampled

before the start of the experiment and after harvest. Additional experimental details are described in Goldberg et al. (2003).

For the field study, soil and plant samples were collected from the Broadview Water District. Soil samples at all sites were collected in the spring. For alfalfa, plants were sampled at ten sites at the time of soil sampling. Muskmelons were sampled at 28 sites prior to fruit set and at maturity. Cotton was sampled at 27 sites at flowering and two subsequent times during the growing season. Additional experimental details are described in Goldberg et al. (2002).

The soil samples were extracted with 1 M ammonium acetate, distilled water, and DTPA-sorbitol. The DTPA-sorbitol extractant contains of 0.005 M diethylenetriaminepentaacetic acid, 0.01 M $CaCl_2$, 0.1 M triethanolamine (TEA) adjusted to pH 7.3, and 0.2 M sorbitol. Boron concentrations in the extracts were determined using inductively coupled plasma (ICP) spectrometry.

In the container study, marginal chlorosis, characteristic of excess B, was found on the melon leaves for all B treatments. Deleterious effects of B on melon growth and development were found. At the highest two B treatments, the number of days to first flowering was significantly delayed, as seen in Figure 14. At the highest B treatment, fruit set was completely inhibited (Goldberg et al., 2003). Similar effects have been observed in pear trees (Crandall et al., 1981) and are a much better indicator of B damage than reductions in dry matter since fruit is the marketable plant part for these crops.

Correlations between various initial soil B concentrations and B content of melon leaves, stems, and fruits at harvest were highly significant for all three extractants. The correlation with fruit B was especially high ($r > 0.99^{**}$). This is very

useful since fruit is the marketable plant part for melons. The ability of the DTPA-sorbitol extractant to predict B content of melon leaves, stems, and fruits is indicated in Figure 15, since this extract showed the highest correlation coefficient.

In the field study, there were significant positive relationships between various extractable soil B concentrations and B content of muskmelon and cotton leaves for all three extractants. For melons, the best correlation was found for the sampling prior to fruit set, in agreement with the recommended sampling protocol for plant analysis. The relationship between melon B and DTPA-sorbitol extractable B is indicated in Figure 16. For cotton, the best correlation was found for the latest plant sampling. This result was surprising since the recommended sampling protocol for cotton is at flowering. The relationship between cotton B and DTPA-sorbitol extractable B is indicated in Figure 17. Despite statistically significant relationships, the predictability of B content in field grown plants is poor using the B DTPA-sorbitol soil test that provided extremely high correlation with plant B content in the container study.

Historically, evaluations of the ability of B soil tests to predict plant B content have been conducted in the greenhouse. These conditions provide a much more controlled environment than the field, where clay and water content and root distribution vary considerably. The much lower, albeit significant, correlations between extractable soil B and plant B observed in the field study are attributed to sampling uncertainties and spatial and temporal fluctuations. These results draw into question the ability of soil B extractants to accurately predict soil solution B concentration experienced by field-grown plants. Soil B extractants that provide good correlation with plant B content in greenhouse studies should also be tested under field conditions.

REFERENCES

Bassett, R.L., 1980, A critical evaluation of the thermodynamic data for B ions, ion pairs, complexes, and polyanions in aqueous solution at 298.15 K and 1 bar, *Geochim. Cosmochim. Acta* 44:1151-1160.

Berger, K.C., and Truog, E., 1940, Boron deficiencies as revealed by plant and soil tests. *J. Am. Soc. Agron.* 32:297-301.

Bingham, F.T., 1982, Boron. In *Methods of soil analysis* (A.L. Page et al., eds.) Agronomy 9, Part 2, 2nd ed., American Society of Agronomy, Soil Science Society of America, Madison, pp 431-447.

Cartwright, B., Tiller, K.B., Zarcinas, B.A., and Spouncer, L.R., 1983, The chemical assessment of the boron status of soils. *Aust. J. Soil Res.* 21:321-332.

Crandall, P.C., Chamberlain, J.D., and Garth, J.K.I., 1981, Toxicity symptoms and tissue levels associated with excess boron in pear trees. *Commun. Soil Sci. Plant Anal.* 12:1047-1057.

Fleming, G.A., 1980, Essential micronutrients. I: Boron and molybdenum. In *Applied soil trace elements* (B.E. Davies, ed.) John Wiley and Sons, New York, pp 155-197.

Goldberg, S., 1992, Use of surface complexation models in soil chemical systems. *Adv. Agron.* 47:233-239.

Goldberg, S., 2005, Inconsistency in the triple layer model description of ionic strength dependent boron adsorption. *J. Colloid Interface Sci.* 285:509-517.

Goldberg, S., 1997, Reactions of boron with soils. *Plant Soil* 193:35-48.

Goldberg, S., Forster, H.S., and Heick, E.L., 1993, Boron adsorption mechanisms on oxides, clay minerals, and soils inferred from ionic strength effects. *Soil Sci. Soc. Am. J.* 57:704-708.

Goldberg, S., Lesch, S.M., and Suarez, D.L., 2000, Predicting boron adsorption by soils using soil chemical parameters in the constant capacitance model. *Soil Sci. Soc. Am. J.* 64:1356-1363.

Goldberg, S., Shouse, P.J., Lesch, S.M., Grieve, C.M., Poss, J.A., Forster, H.S., and Suarez, D.L., 2002, Soil boron extractions as indicators of boron content of field-grown crops. *Soil Sci.* 67:720-728.

Goldberg, S., Shouse, P.J., Lesch, S.M., Grieve, C.M., Poss, J.A., Forster, H.S., and Suarez, D.L., 2003, Effect of high boron application on boron content and growth of melons. *Plant Soil* 256:403-411.

Goldberg, S., Suarez, D.L., Basta, N.T. and Lesch, S.M., 2004, Predicting boron adsorption isotherms by Midwestern soils using the constant capacitance model. *Soil Sci. Soc. Am. J.* 68:795-801.

Gupta, S.K., and Stewart, J.W.B., 1974, The extraction and determination of plant-available boron in soils. *Schweiz. Landwirtsch. Forsch.* 14:153-159.

Gupta, U.C., 1968, Relationship of total and hot-water soluble boron, and fixation of added boron, to properties of Podzol soils. *Soil Sci. Soc. Am. Proc.* 32:45-48.

Hunter, R.J., 1981, *Zeta potential in colloid science. Principles and applications.* Academic Press, London.

Keren, R., Bingham, F.T., and Rhoades, J.D., 1985, Plant uptake of boron as affected by boron distribution between liquid and solid phases in soil. *Soil Sci. Soc. Am. J.* 49:297-302.

Keren, R., and Mezuman, U., 1981, Boron adsorption by clay minerals using a phenomenological equation. *Clays Clay Miner.* 29:198-203.

McBride, M.B., 1997, A critique of diffuse double layer models applied to colloid and

surface chemistry. *Clays Clay Miner.* 45:598-608.

Miller, R.O., Vaughan, B., and Kotuby-Amacher, J., 2000, Extraction of soil boron with DTPA-sorbitol. *Soil-Plant Anal.* Spring:4-10.

Peak, D., Luther, G.W., and Sparks, D.L., 2003, ATR-FTIR spectroscopic studies of boric acid adsorption on hydrous ferric oxide. *Geochim. Cosmochim. Acta* 67:2551-2560.

Su, C., and Suarez, D.L., 1995, Coordination of adsorbed boron: A FTIR spectroscopic study. *Environ. Sci. Technol.* 29:302-311.

Su, C., and Suarez, D.L., 1997, Boron sorption and release by allophane. *Soil Sci. Soc. Am. J.* 61:69-77.

Su, C., and Suarez, D.L., 2004, Boron release from weathering of illites, serpentine, shales, and illitic/palygorskitic soils. *Soil Sci. Soc. Am. J.* 68:96-105.

Suarez, D.L., and Simunek, J., 1997, UNSATCHEM: Unsaturated water and solute transport model with equilibrium and kinetic chemistry. *Soil Sci. Soc. Am. J.* 61:1633-1646.

FIGURES

Figure 1. Electrophoretic mobility of the aluminum oxide, gibbsite as a function of total solution B concentration and pH. From Goldberg et al. (1993).

Figure 2. Boron adsorption on the iron oxide, goethite as a function of solution ionic strength and pH. Adapted from Goldberg et al. (1993).

Figure 3. Dissociation of boric acid.

Figure 4. ATR-FTIR spectra of aqueous boric acid as a function of solution pH and total B concentration. From Su and Suarez (1995).

Figure 5. ATR-FTIR difference spectra of B adsorbed onto amorphous aluminum oxide as a function of pH and equilibrium boron concentration. From Su and Suarez (1995).

Figure 6. ATR-FTIR difference spectra of B adsorbed onto amorphous iron oxide as a function of pH and equilibrium boron concentration. From Su and Suarez (1995).

Figure 7. ATR-FTIR spectra of boron adsorbed on the hydrous iron oxide surface at pH 6.5 and I = 0.01 M as a function of initial boron concentrations (from bottom: 0, 50, 100, 500, and 100 μM). From Peak et al. (2003).

Figure 8. Cumulative B extracted as a function of sequential aqueous extraction for various minerals (12 h, 1:10 w/v with 0.1 M $CaCl_2$ for the first three extractions and 0.01 M $CaCl_2$ for subsequent extractions). From Su and Suarez (2004).

Figure 9. Effect of particle size, pH, and time on B concentration and B release from a soil from the San Joaquin Valley of California, USA. From Su and Suarez (2004).

Figure 10. Placement of ions, charge, surface charge, σ, and surface potential, ψ for the constant capacitance model.

Figure 11. Fit of the constant capacitance model to B adsorption: (a) Diablo clay; (b) Fallbrook subsoil. Circles represent experimental data. Model fits are represented by solid lines. From Goldberg et al. (2000).

Figure 12. Constant capacitance model prediction of B adsorption by southwestern USA soils not used to obtain the prediction equations. Circles represent experimental data. Model predictions are represented by solid lines. Adapted from Goldberg et al. (2000).

Figure 13. Constant capacitance model prediction of B adsorption by Midwestern USA soils not used to obtain the prediction equations: (a) Mansic soil; (b) Osage soil; (c) Pond Creek soil; (d) Summit soil. Circles represent experimental data. Model predictions are represented by solid lines. Adapted from Goldberg et al. (2004).

Figure 14. Delay in flowering of melons as a function of B treatment. Error bars represent one standard deviation from the mean of four replicates per treatment. From Goldberg et al. (2003).

Figure 15. Ability of DTPA-sorbitol extractable B to predict B content of melons: (a) leaf B; (b) stem B; (c) fruit B. Error bars represent one standard deviation from the mean of eight plants per treatment. From Goldberg et al. (2003).

Figure 16. Boron content of melon plants prior to fruit set as a function of DTPA-sorbitol extractable soil B content depth averaged over the root zone (0-90 cm). From Goldberg et al. (2002).

Figure 17. Boron content of cotton leaves at the end of the growing season as a function of DTPA-sorbitol extractable soil B content depth averaged over the root zone (0-180 cm). From Goldberg et al. (2002).

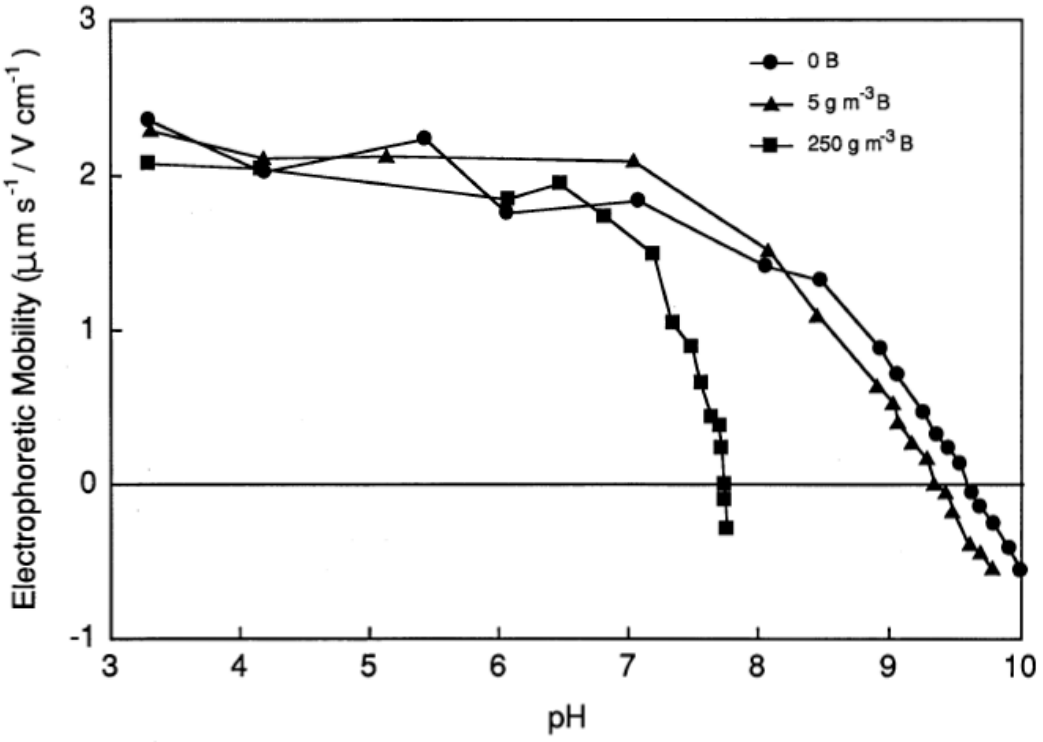
Electrophoretic Mobility (μm s-1 / V cm-1)
pH
0 B
5 g m-3 B
250 g m-3 B
3
2
1
0
-1
3
4
5
6
7
8
9
10

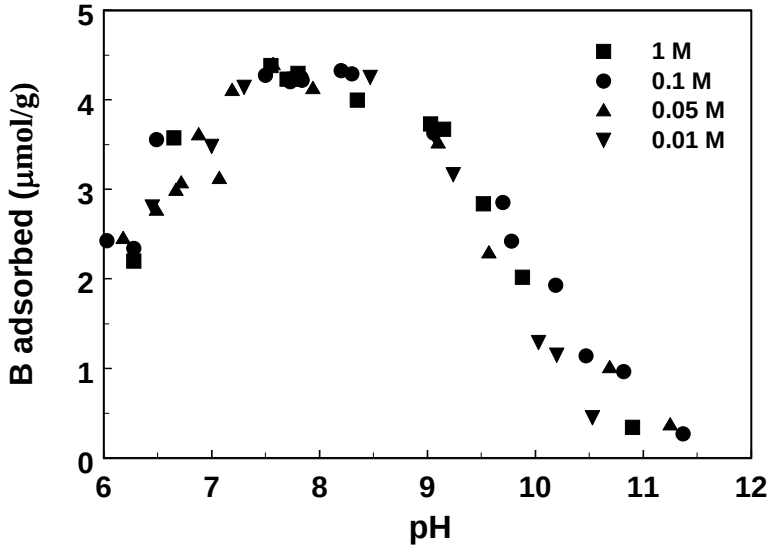
B adsorbed (μmol/g)
pH
1 M
0.1 M
0.05 M
0.01 M
0
1
2
3
4
5
6
7
8
9
10
11
12

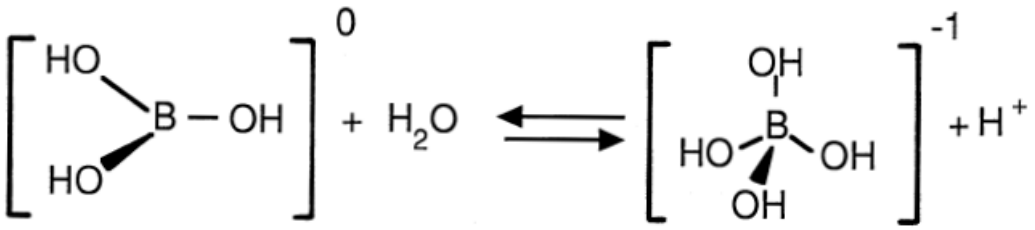

Boric Acid
Trigonal

Borate Anion
Tetrahedral

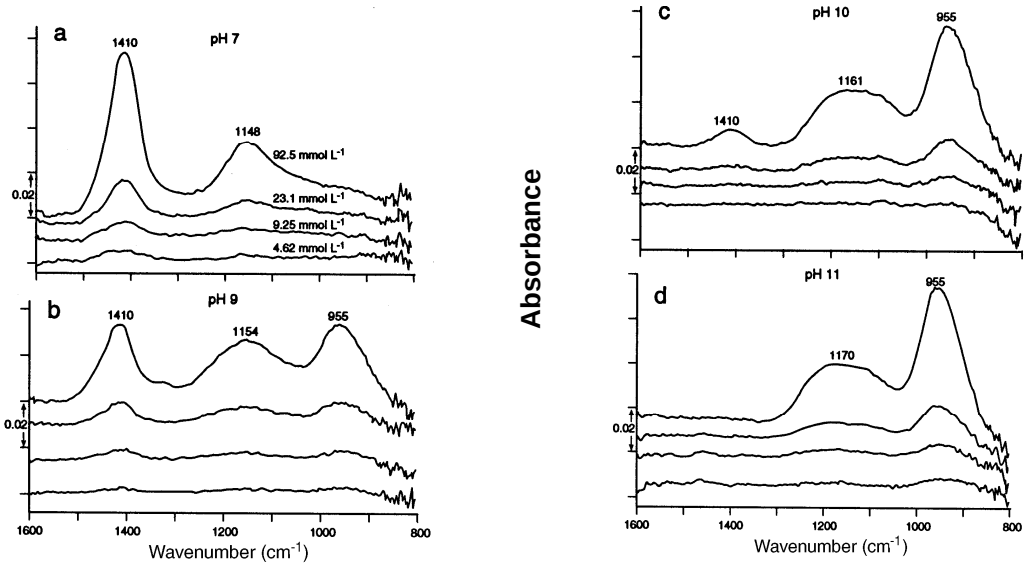
a
pH 7
1410
1148
92.5 mmol L-1
23.1 mmol L-1
9.25 mmol L-1
4.62 mmol L-1
0.02
b
pH 9
1410
1154
955
0.02
1600
1400
1200
1000
800
Wavenumber (cm-1)
Absorbance
c
pH 10
955
1161
1410
0.02
d
pH 11
955
1170
0.02
1600
1400
1200
1000
800
Wavenumber (cm-1)

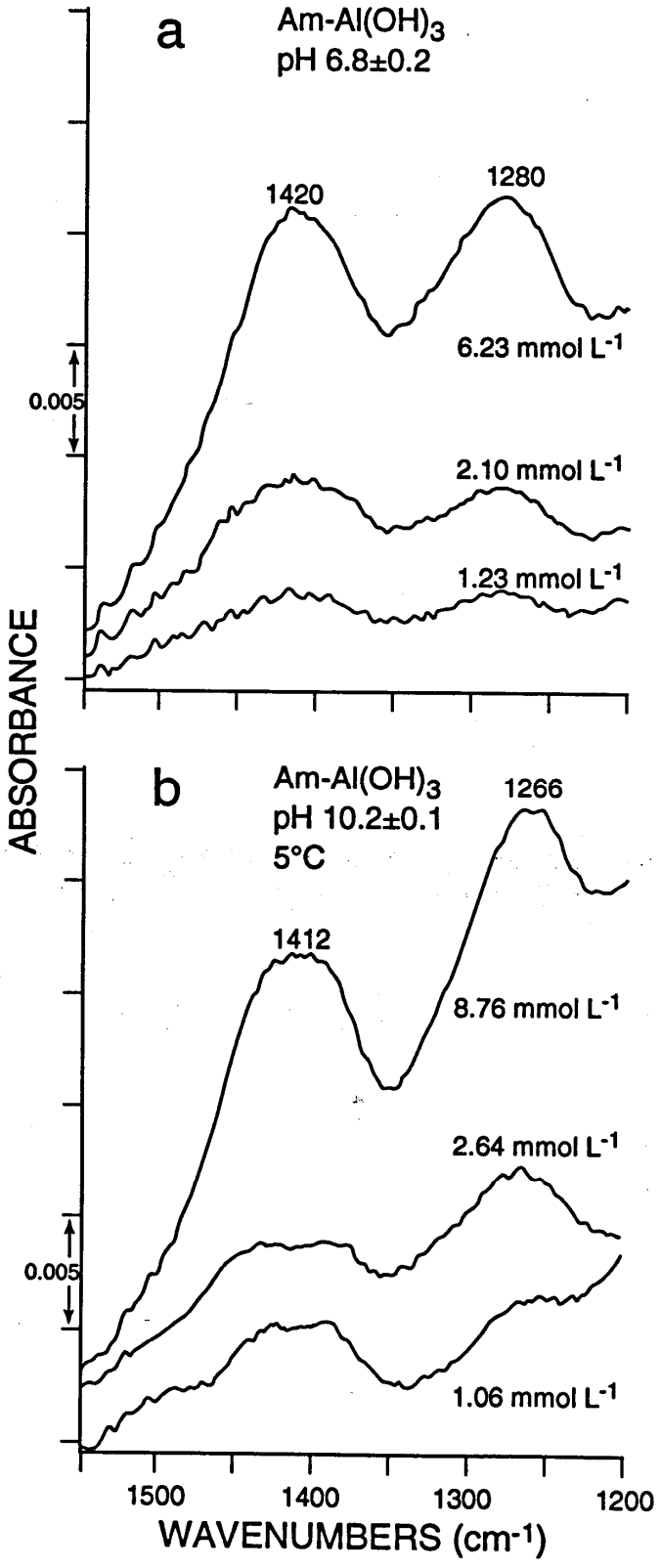
a
Am-Al(OH)3
pH 6.8±0.2
1420
1280
6.23 mmol L-1
0.005
2.10 mmol L-1
1.23 mmol L-1
ABSORBANCE
b
Am-Al(OH)3
pH 10.2±0.1
5°C
1266
1412
8.76 mmol L-1
2.64 mmol L-1
0.005
1.06 mmol L-1
1500
1400
1300
1200
WAVENUMBERS (cm-1)

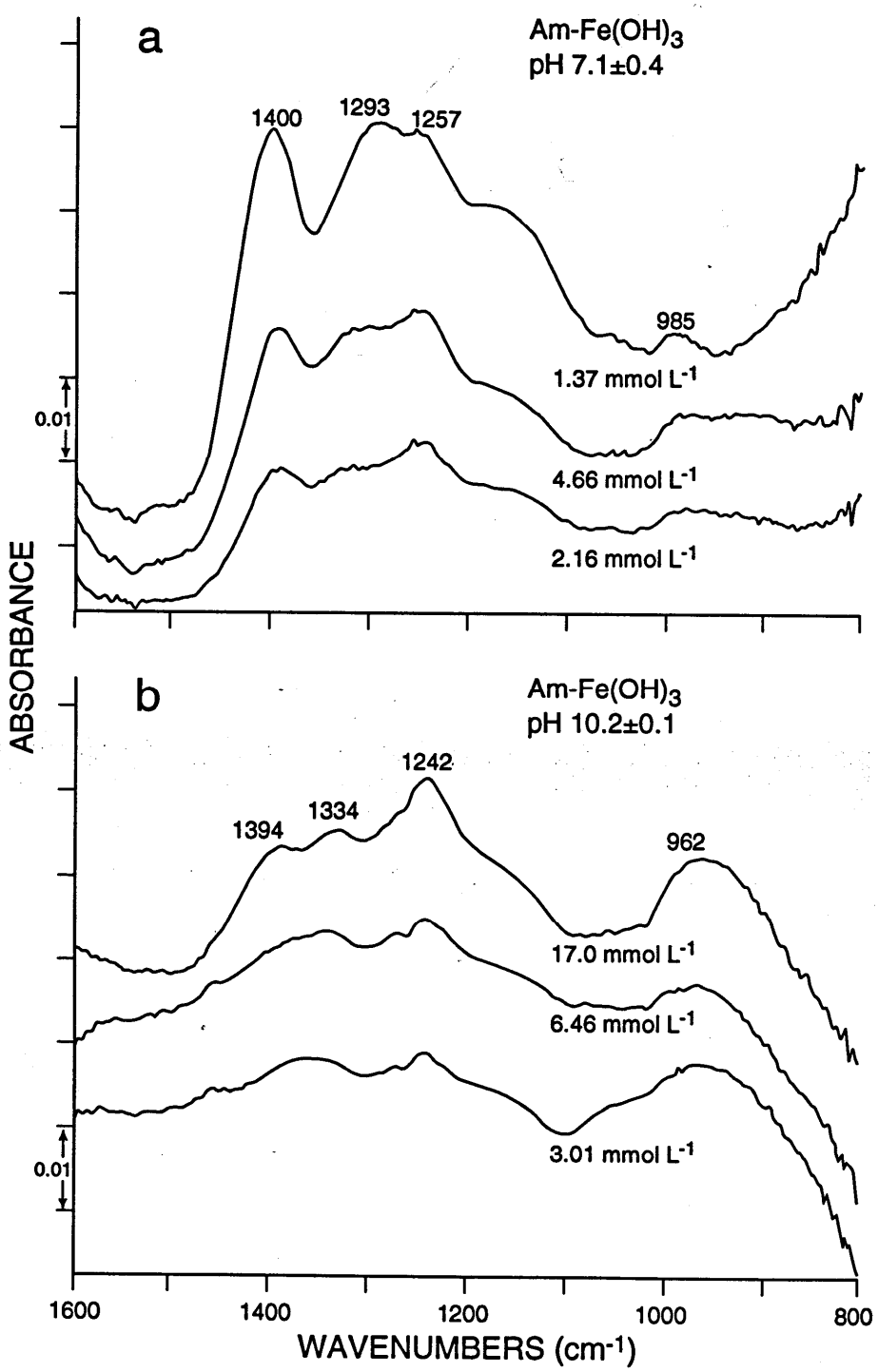
a
Am-Fe(OH)3
pH 7.1±0.4
1400
1293
1257
985
1.37 mmol L-1
4.66 mmol L-1
2.16 mmol L-1
0.01
b
Am-Fe(OH)3
pH 10.2±0.1
1242
1394
1334
962
17.0 mmol L-1
6.46 mmol L-1
3.01 mmol L-1
0.01
ABSORBANCE
1600
1400
1200
1000
800
WAVENUMBERS (cm-1)

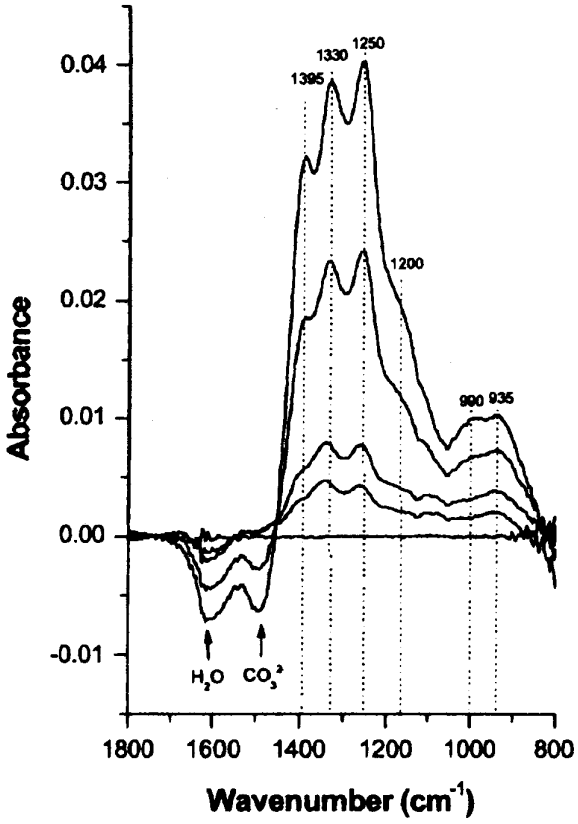
0.04
0.03
0.02
0.01
0.00
-0.01
Absorbance
1395
1330
1250
1200
990
935
H2O
CO3 2
1800
1600
1400
1200
1000
800
Wavenumber (cm-1)

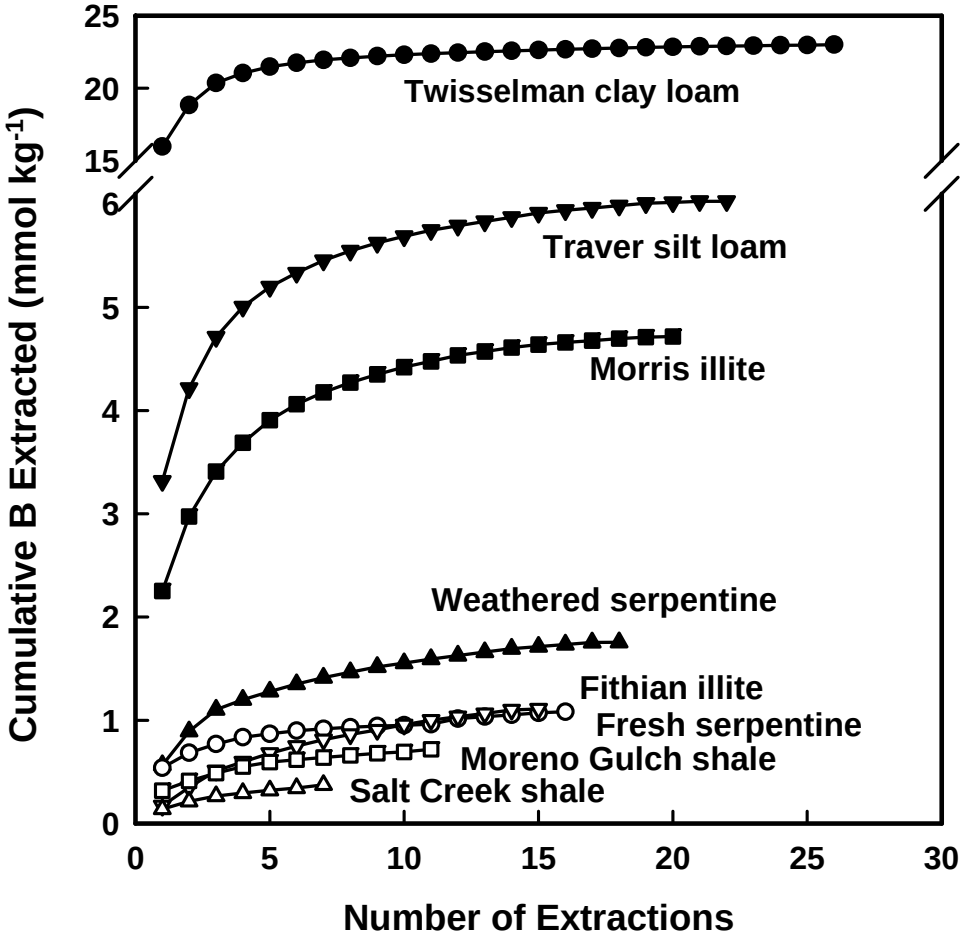
Cumulative B Extracted (mmol kg-1)
Number of Extractions
Twisselman clay loam
Traver silt loam
Morris illite
Weathered serpentine
Fithian illite
Fresh serpentine
Moreno Gulch shale
Salt Creek shale
0
1
2
3
4
5
6
15
20
25
0
5
10
15
20
25
30

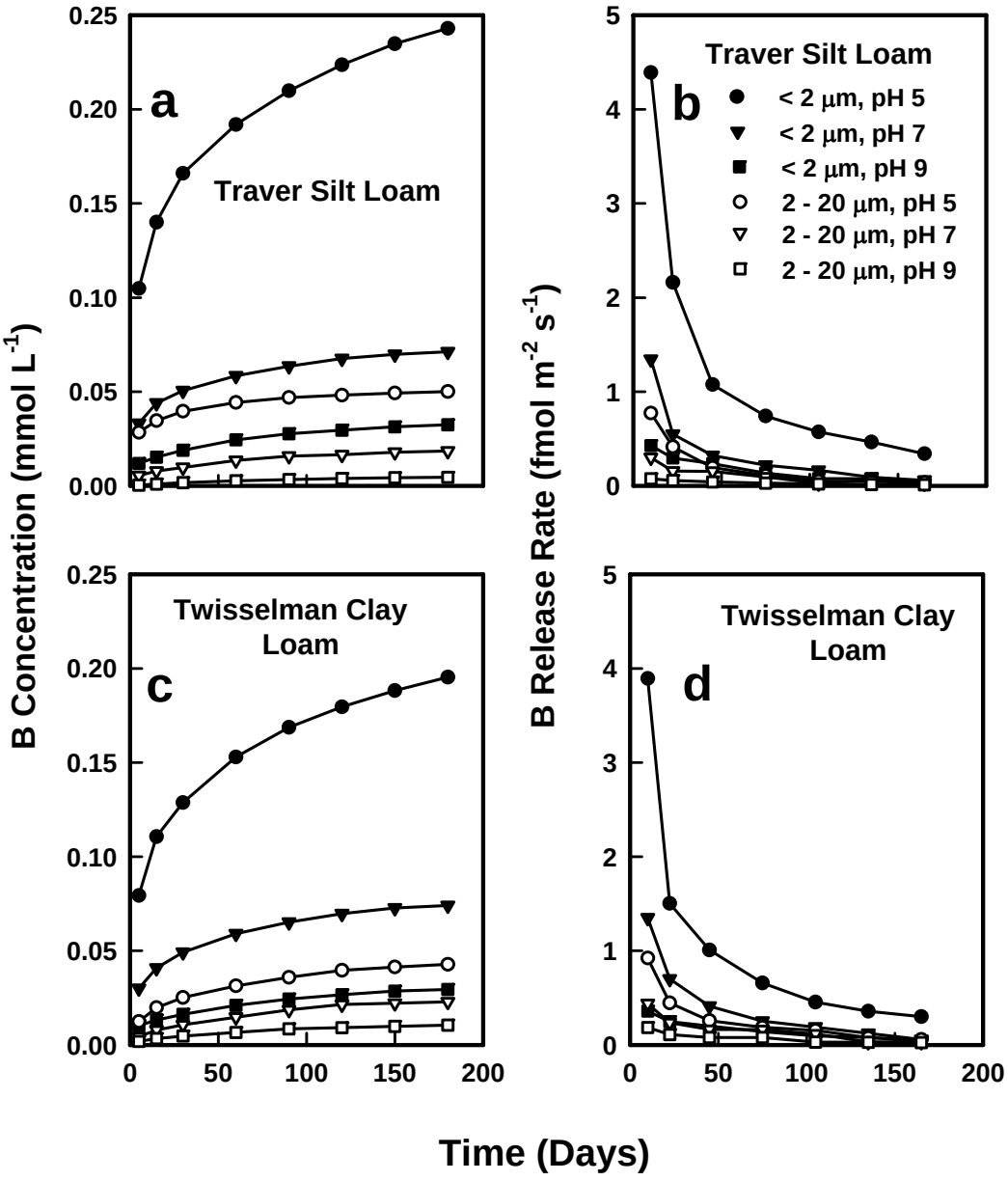
a
Traver Silt Loam
b
Traver Silt Loam
< 2 μm, pH 5
< 2 μm, pH 7
< 2 μm, pH 9
2 - 20 μm, pH 5
2 - 20 μm, pH 7
2 - 20 μm, pH 9
c
Twisselman Clay Loam
d
Twisselman Clay Loam
B Concentration (mmol L-1)
B Release Rate (fmol m-2 s-1)
Time (Days)
0.25
0.20
0.15
0.10
0.05
0.00
5
4
3
2
1
0
0
50
100
150
200

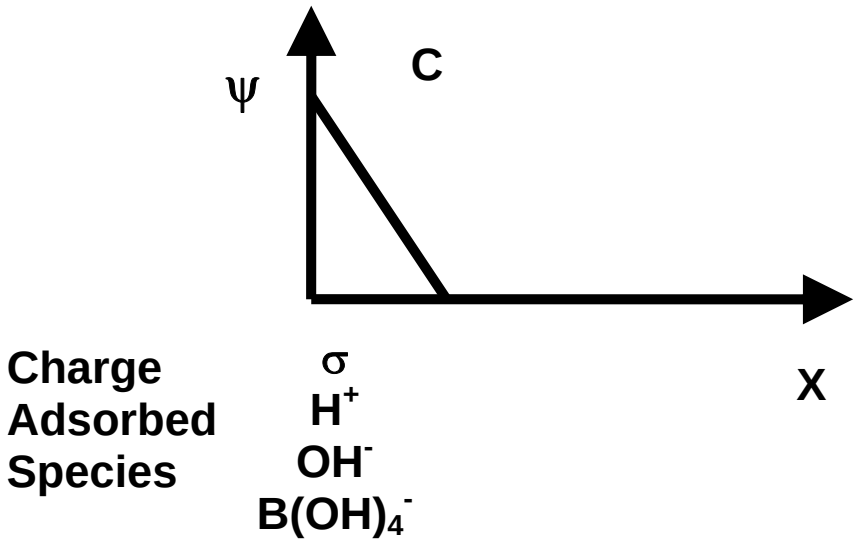
ψ
C
X
Charge
Adsorbed
Species
σ
H+
OH-
B(OH)4-

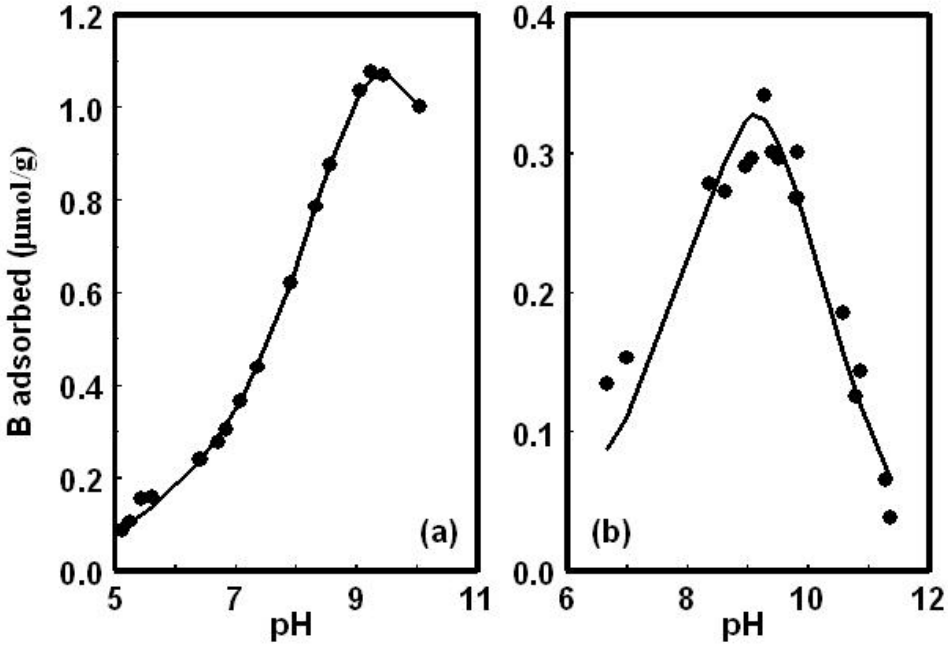
B adsorbed (µmol/g)
1.2
1.0
0.8
0.6
0.4
0.2
0.0
5
7
9
11
pH
(a)
0.4
0.3
0.2
0.1
0.0
6
8
10
12
pH
(b)

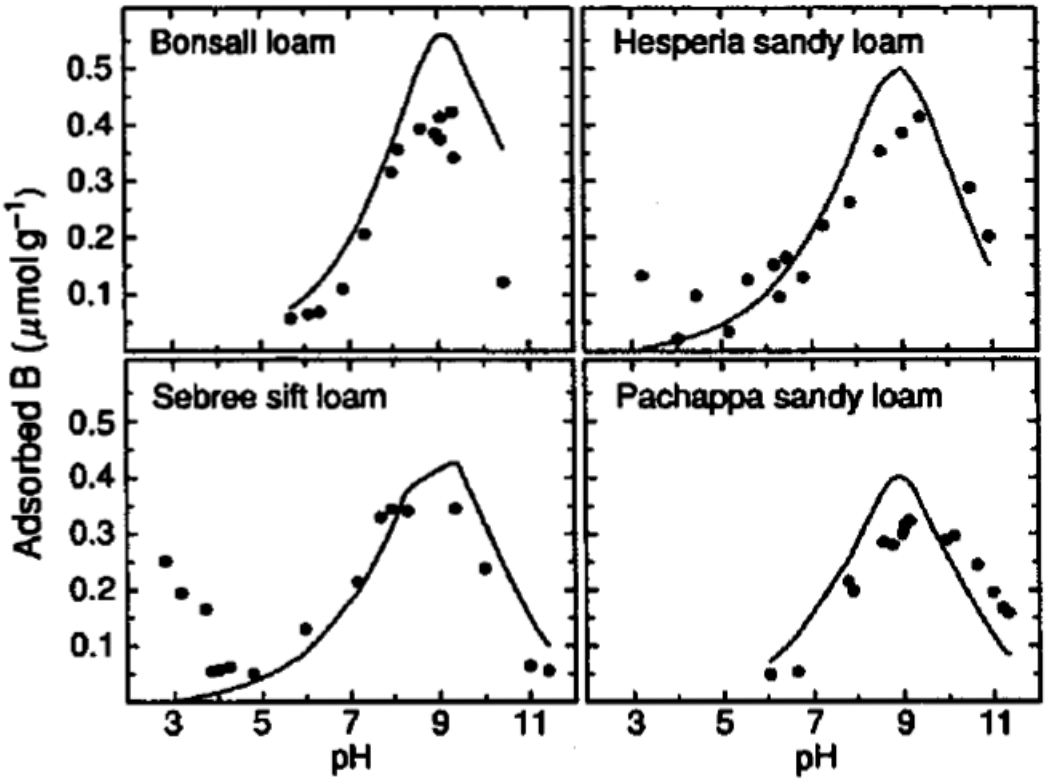
Bonsall loam
Hesperia sandy loam
Sebree sift loam
Pachappa sandy loam
Adsorbed B (μmol g⁻¹)
0.5
0.4
0.3
0.2
0.1
3
5
7
9
11
pH

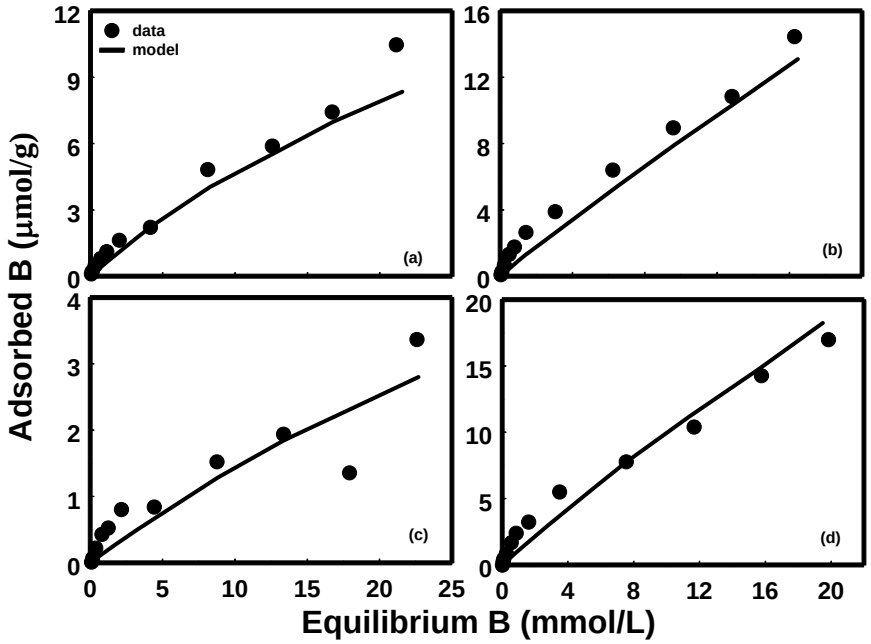
data
model
(a)
(b)
(c)
(d)
Adsorbed B (μmol/g)
Equilibrium B (mmol/L)

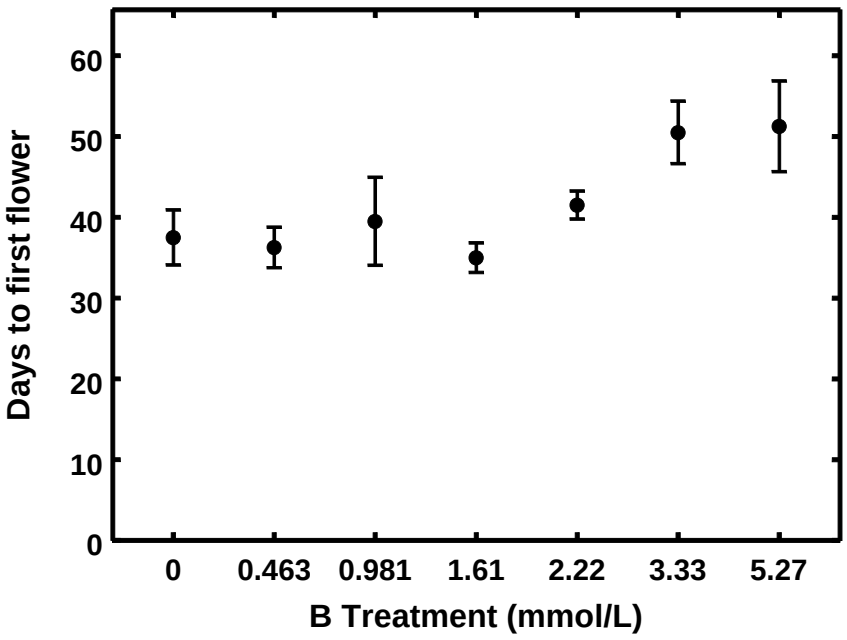
Days to first flower
60
50
40
30
20
10
0
0
0.463
0.981
1.61
2.22
3.33
5.27
B Treatment (mmol/L)

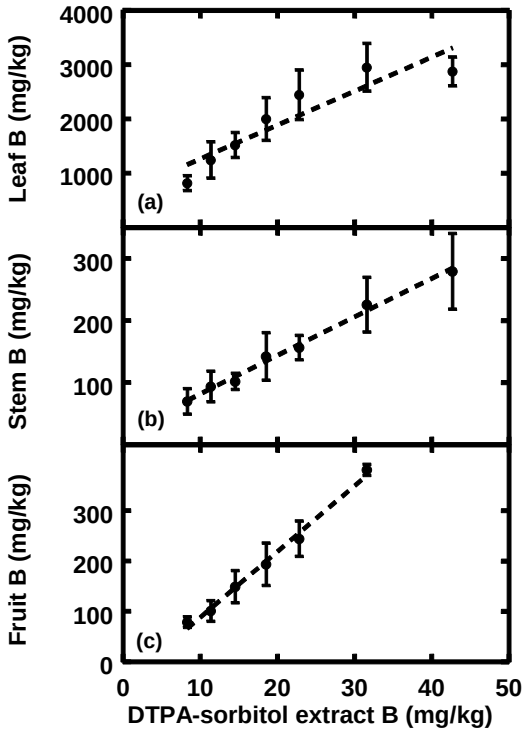
Leaf B (mg/kg)
4000
3000
2000
1000
(a)
Stem B (mg/kg)
300
200
100
(b)
Fruit B (mg/kg)
300
200
100
0
(c)
0
10
20
30
40
50
DTPA-sorbitol extract B (mg/kg)

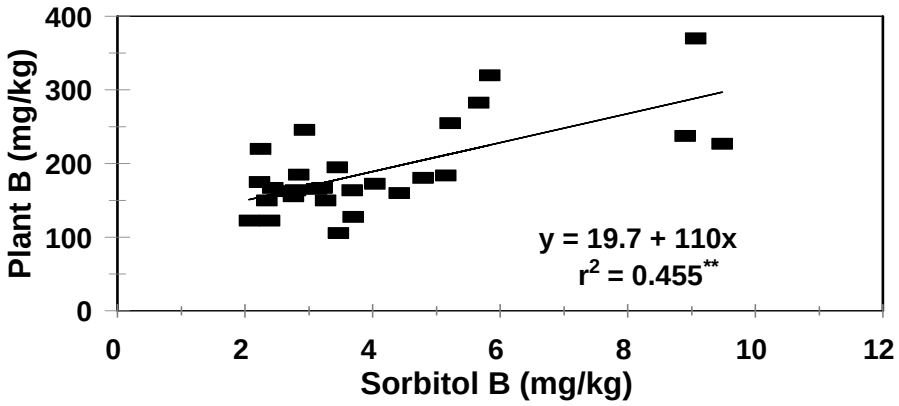
Plant B (mg/kg)
400
300
200
100
0
0
2
4
6
8
10
12
Sorbitol B (mg/kg)
y = 19.7 + 110x
r2 = 0.455**

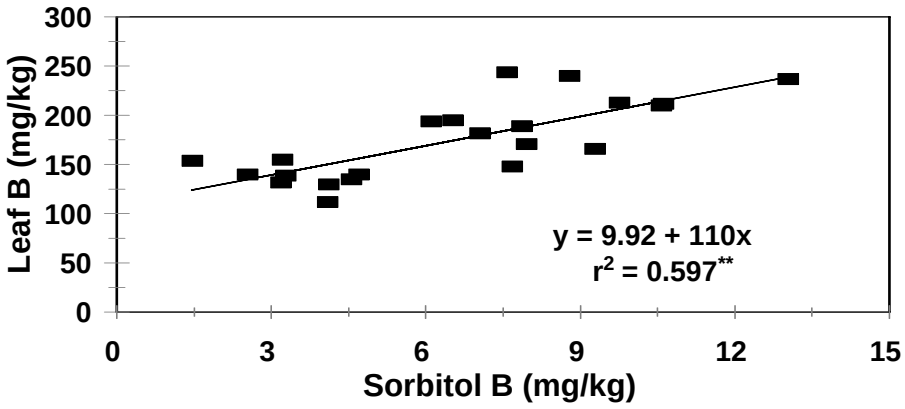
300
250
200
150
100
50
0
Leaf B (mg/kg)
0
3
6
9
12
15
Sorbitol B (mg/kg)
y = 9.92 + 110x
r2 = 0.597**